



## Protective and Therapeutic Effects of *Houttuynia cordata* for Vitiligo Induced by Oxidative Stress and Hydroquinone

Badmaarag-Altai Chuluunbaatar<sup>1</sup>, Se-woong Kim<sup>1</sup>, and Yunjo Soh<sup>1,\*</sup>

<sup>1</sup>Laboratory of Pharmacology, School of Pharmacy, Jeonbuk National University, Jeonju 54907 Republic of Korea

**Abstract** – Vitiligo is a type of chronic autoimmune skin disorder that is highly unpredictable. *Houttuynia cordata* Thunb. (HC) is a natural compound with several pharmacological properties; however, the fundamental mechanisms of HC effects on Vitiligo have yet to be fully understood. This study aimed to evaluate the effects of HC on the oxidative injury of melanocytes *in vivo* and *in vitro*. This study demonstrated that compounds significantly prevented the hydrogen peroxide (H<sub>2</sub>O<sub>2</sub>)-induced B16F10 cell loss of viability and melanin synthesis; in addition, cell apoptosis-regulating of melanocytes significantly decreased, and the expression level of TRP-1 and MITF increased dose-dependently. In animal experiments, C57BL/6 mice received 5% hydroquinone (HQ) for 5 weeks and were treated with HC for 2 weeks. HQ-stimulated vitiligo in mice also produced melanocyte and melanosome degradation. The melanin content and tyrosinase activity of the mice (skin) that received the HC group significantly increased compared to the untreated and 8-methoxyprosalen (8-MOP) groups. These experiments suggest that the HC has potential protective and therapeutic effects for vitiligo.

**Keywords** – *Houttuynia cordata*, Vitiligo, Melanin, Apoptosis, Oxidative stress, Hydroquinone

### Introduction

Vitiligo is a chronic autoimmune disease characterized by dysfunctional melanocytes.<sup>1</sup> Pale milk-white patches resulting from the selective loss of melanocytes are clinically distinctive indications of vitiligo.<sup>2</sup> The pathophysiology is still unclear as to exactly what causes vitiligo. However, through several potential pathways, including loss of functional melanocytes due to oxidative stress, metabolic irregularities, melanocyte detachment mechanisms, production of inflammatory mediators, and autoimmune responses.<sup>2,3</sup>

Melanin plays a role in the pigmentation synthesis of the skin and is produced by melanosomes in melanocytes, which transport melanosomes to binding keratinocytes located in the epidermal-dermal junction.<sup>4</sup> Melanin molecules absorb radiation and prevent damage to the skin. However, high levels of intracellular ROS are created as a side product during melanogenesis. This makes melanocytes relatively more susceptible to the risk of oxidative stress.<sup>5</sup> Oxidative stress plays an important role in the assault and progression of vitiligo.<sup>6</sup> Melanogenesis is the biochemical process of melanin synthesis within melanosomes and is regulated by

tyrosinase (TYR), tyrosinase-related protein-1 (TRP-1), and TRP-2.<sup>7,8</sup> Microphthalmia-associated transcription factor (MITF) promotes melanocyte proliferation and development and is an important regulator of melanogenic key enzymes such as TYR, TRP-1, and TRP-2.<sup>9,10</sup> Bcl-2 and Bax are key proteins involved in the regulation of apoptosis, which also indirectly affects melanogenesis.<sup>11</sup> Bcl-2 protein expression inhibits cell death promoted by oxidative stress<sup>12</sup>, while Bax is a pro-apoptotic molecule that induces apoptosis<sup>13</sup>. This indicates a potential role for these proteins in the death mechanism of melanocytes in vitiligo.<sup>14</sup>

*Houttuynia cordata* Thunb. (HC) is a medical plant often discovered in Southeast Asia. Previous studies have shown that polysaccharides, fatty acids, polyphenols, flavonoids, and sterols are found in HC extracts. Natural extracts pharmacologically possess anti-oxidative, anti-inflammatory, antiviral, antibacterial, and antitumor qualities.<sup>15,16</sup> Polyphenols play an important role in antioxidants that neutralize free radicals, protecting cells from damage and helping to prevent chronic disease.<sup>17</sup> However, there were no reports of HC compounds in natural extracts for vitiligo, and the protective impact of melanogenesis and oxidative stress *in vivo* and *in vitro* is not fully understood. Therefore, this study determines the effect of HC extract on melanocytes against apoptosis-induced oxidative injury elucidated in animal models and B16F10 murine melanoma cells.

\*Author for correspondence

Yunjo Soh, Ph. D., Laboratory of Pharmacology, School of Pharmacy, Jeonbuk National University, Jeonju 54907 Republic of Korea  
Tel: +82-63-270-4038; E-mail: ysoh@jbnu.ac.kr

## Experimental

**Materials** – The *Houttuynia cordata* Thunb. (HC) plant was ultrasonically extracted with 30% ethanol for 1 hour, then extracted twice through filtration after decompressing and concentrating. The extract has been freeze-dried. Dulbecco's modified Eagle's medium (DMEM), fetal bovine serum (FBS), penicillin, and streptomycin were purchased from Gibco (NY, USA). B16F10 melanoma cells were purchased from the American Type Culture Collection ATCC (Manassas, VA, USA). The hydroquinone (HQ H9003), 8-methoxyprosalen (8-MOP M3501), 3,4-dihydroxy-L-phenylalanine (L-DOPA D9628), Alpha-melanocyte stimulating hormone ( $\alpha$ -MSH M4135), phosphatase inhibitor cocktail (P0044), sodium hydroxide solution (NaOH S2770), and hydrogen peroxide solution ( $H_2O_2$  H1009) were acquired from Sigma-Aldrich (St. Louis, MO, USA). Anti-MITF (1:1000 ab303530), TRP-1 (1:10000 ab178676), Bax (1:1000 #2772), and Bcl-2 (1:1000 #4223) primary antibodies were obtained from Abcam (Cambridge, MA, USA) and Cell Signaling Technology (Danvers, MA, USA).  $\beta$ -actin (sc-477778) and anti-mouse, anti-rabbit secondary antibodies were purchased from Santa Cruz Biotechnology (Dallas, TX, USA).

**Cell culture** – B16F10 mouse skin melanoma cells were cultured in a standard Dulbecco's modified Eagle's medium (DMEM high glucose) supplemented with 10% fetal bovine serum (FBS), penicillin (100 U/mL), and streptomycin (100  $\mu$ g/mL) and incubated at 37°C in an atmosphere containing 95% air and 5%  $CO_2$ .

**Cell viability assay** – Cell viability was determined by the CCK-8 assay. B16F10 melanoma cells were incubated for 24 h in the cell culturing medium. The cells ( $4 \times 10^3$  cells/well) were seeded into 96-well plates separately and treated with various HC and chemical doses for 24 h. After incubation, the cells were induced with  $H_2O_2$  at 1 mM for 4 h. The supernatant was removed, and 10  $\mu$ L of CCK-8 was added to each well of cell medium and cultured for 1–4 h. Then it was quantified with a microplate reader at 450 nm.

**Measurement of Melanin Content** – The amount of melanin in the cells was determined by slightly altering previously described methods.<sup>18</sup>  $1 \times 10^5$  B16F10 cells per well were seeded on 6-well plates and incubated for 24 h in the culture medium. HC (100  $\mu$ g/mL) and  $\alpha$ -MSH (100 nM) were treated for 24 h.  $\alpha$ -MSH was used as the positive control treatment. After incubation, the cells were induced with  $H_2O_2$  at 1 mM for 4 h. The cell pellets were harvested and dissolved in 1 N NaOH at 80°C for 1 h. The melanin content was analyzed at 405 nm using a microplate reader. For the tissue melanin assay, tissues were equally weighed

before boiling in 1 N NaOH for 90 min. The supernatants were separated by centrifugation at 13,000 rpm for 20 min, and then the sample was measured for melanin content as previously described.

**Tyrosinase Activity** – The tyrosinase activity was measured by the rate of L-3, 4-dihydroxyphenylalanine (L-DOPA) oxidase activity, as described by the method with a lightly modified.<sup>19</sup> B16F10 cells seeded in 6-well plates ( $1 \times 10^5$  cells/well) were pre-treated with HC (100  $\mu$ g/mL) and  $\alpha$ -MSH (100 nM) for 24 h, then further incubated with 1 mM of  $H_2O_2$  for 4 h. Cells were harvested to determine cellular tyrosinase activity, and the supernatant was discarded. Pellets were washed with ice-cold PBS and lysed with 1x RIPA (200  $\mu$ L) buffer containing a 1% protease inhibitor cocktail at 4°C for 20 min. The lysate was centrifuged at 13,000 rpm for 20 min at 4°C to obtain a supernatant of 90  $\mu$ L, and 10  $\mu$ L of L-DOPA (10 mM) was added in 96-well plates and incubated at 37°C for 2 h. Then it was quantified with a microplate reader at 475 nm. Tissues were weighed evenly before being lysed with RIPA at 4°C for 30 minutes, and tyrosinase activity was determined as previously described.

**Western blot analysis** – B16F10 cells were cultured in 100-mm dishes and treated with various concentrations of HC (25, 50, and 100  $\mu$ g/mL) and  $\alpha$ -MSH (100 nM) for 24 h, then further incubated with 1 mM of  $H_2O_2$  for 4 h. Cells were lysed with RIPA buffer and a 1% phosphatase inhibitor cocktail at 4°C and vortexed every 10 min for 1 h. After centrifugation at 13,000 rpm for 20 min, the harvested supernatant and proteins were quantified through a BCA assay. The calculated proteins from each sample were diluted in Laemmli buffer 4x and boiled for 5 min at 95°C. Polyacrylamide gels (10%) were loaded with 20–40  $\mu$ g of samples to separate proteins, and these isolated proteins were transferred to polyvinylidene fluoride (PVDF) membranes. 5% nonfat skimmed milk in Tris-buffered saline containing 0.4% Tween 20 (TBST), which was blocked to prevent nonspecific antibody bindings for 1 h at room temperature. Blocked membranes with primary antibodies were incubated at 4°C overnight. Secondary conjugated antibodies were diluted at 1:3000 for 2 hours at room temperature. Protein expressions were developed using an ECL detection kit.

**Animals** – The ethics committee for animal handling at Jeonbuk National University, South Korea, approved the study. All mouse experiments were performed according to the local institutional Animal Care and Use Committee (IACUC) guidelines. C57BL/6 mice ( $20 \pm 5$  g, 5 weeks) were obtained from Nara Biotech Pyeongtaek Plant (Gyeonggi-do, Korea). All mice were housed on a 12-hour light and 12-hour dark schedule in humid conditions ( $50 \pm 10\%$ ) and were single-housed with water

and food for 5 weeks in standard plastic cages at 24°C–26°C.

**Experimental animal timeline design and treatment** – C57BL/6 mice were divided into 4 groups: the untreated control group was administered distilled water and smeared for 5 weeks ( $n = 4$ ). The vehicle group received 5% (HQ) of the shaved dorsum for 5 weeks and was administered distilled water for 2 weeks ( $n = 4$ ). The 8-MOP group (4.25 mg/kg) ( $n = 4$ ) and the HC group (100 mg/kg) ( $n = 4$ ). All treatment groups received 5% HQ for 5 weeks; each drug was administered orally once every 24 hours for 2 weeks. The intramuscular injection for anesthesia was 20 mg/kg of Zoletil 50 (Laboratoires Virbac, Carros, France) after the shaved dorsum. All mice were sacrificed after 5 weeks when dorsum skin samples were collected.

**Histomorphometric analysis** – Mice dorsal skin samples were isolated and fixed with 10% formalin-containing 0.1 M phosphate buffer at a pH of 7.4. After fixation, tissues were washed in PBS, dehydrated in graded alcohols, and embedded in paraffin. Tissues were sectioned at 5  $\mu\text{m}$  using a cryostat, stained with hematoxylin and eosin (H&E), and mounted on microscope glass slides. The skin thickness was measured three times (average) in each sample, together with the epidermal ridge and dermal papillae<sup>20</sup>, then quantified by Image J software.

**Statistical analysis** – All experiments were conducted three times, and a one-way ANOVA with Tukey's multiple comparisons test was used to determine the results. The data are presented as mean  $\pm$  SD and were analyzed in all statistical tests using the GraphPad Prism software program (GraphPad Prism Inc., La Jolla, CA, USA). A value of  $p < 0.05$  is considered statistically significant.

## Results and Discussion

The CCK-8 assay was used to assess the cytotoxic effect of HC on B16F10 melanoma cells. Cells were treated with HC doses ranging from 1.5625 to 100  $\mu\text{g}/\text{mL}$  for 24 h. Figure 1A shows no cytotoxicity in B16F10 cells treated with HC at various doses, even at the highest concentration (100  $\mu\text{g}/\text{mL}$ ), which did not show obvious cytotoxic effects. As shown in Fig. 1, the cell viability decreased by 50% following exposure to 1 mM  $\text{H}_2\text{O}_2$  for 4 h. These results suggested that HC exhibited protective effects on oxidatively stressed melanoma cells.

To explore the effect of HC on the up-regulation of tyrosinase activity and melanin synthesis by measuring melanin content in B16F10 cells with  $\text{H}_2\text{O}_2$ -induced oxidative stress. As shown in Fig. 2, cells were pretreated with HC (100  $\mu\text{g}/\text{mL}$ ) for 24 h, and induced  $\text{H}_2\text{O}_2$  for 4 h significantly upregulated tyrosinase activity, and melanin content was significantly increased compared to

the untreated and  $\alpha$ -MSH groups. These results indicate that HC potential protects and significantly increases melanin synthesis and tyrosinase upregulation in B16F10 cells.

The effects of HC on the function of melanocytes after treatment with  $\text{H}_2\text{O}_2$  were examined through the expression of MITF and TRP-1, which act as transcription regulators in the melanogenesis process. The B16F10 cells were treated with 25  $\mu\text{g}/\text{mL}$ , 50  $\mu\text{g}/\text{mL}$ , and 100  $\mu\text{g}/\text{mL}$  HC for 24 h and 1 mM  $\text{H}_2\text{O}_2$  for 4 h, respectively. Results indicated that HC protected and improved the expression of MITF and TRP-1, which suggested that HC potential protects and promotes melanogenesis by increasing the expression of these proteins (Fig. 3A–C).

To examine the protective effect of HC against  $\text{H}_2\text{O}_2$ -induced apoptosis, B16F10 cells were pretreated with various concentrations of HC (25, 50, and 100  $\mu\text{g}/\text{mL}$ ), and positive control ( $\alpha$ -MSH) for 24 h before 1.0 mM  $\text{H}_2\text{O}_2$  was added. As shown in Fig. 3D and E, compared with the untreated and positive control groups, the expression of Bcl-2 protein was increased and the expression of Bax protein was inhibited. This indicated that HC revealed the potential to protect melanocyte cell death from induced oxidative stress.

The black hair of the C57BL/6 mouse indicated that it contained more melanin particles.<sup>21,22</sup> Therefore, to explore the impact of the HC treatment group on melanogenesis, we selected the HQ-induced C57BL/6 mice model. HQ-induced mice started visible whitening of the dorsal skin and hair in the third week of the experiment. The dorsal skin significantly increased in progressive darkening after HC oral treatment for 2 weeks (Fig. 4A, B). The depigmentation was quantified blindly in the experimental groups using a point scale based on the extent of depigmentation at dorsal locations.<sup>23</sup> The following was the distribution of points: 0% of the population showed no signs of depigmentation, so the score was 0, > 0–10% = 1 point, > 10–25% = 2 points, > 25–75% = 3 points, > 75–<100% = 4 points, and 100% = 5 points.<sup>24</sup> The average individual score of every mouse in an experimental group is presented as the group's Vitiligo score.<sup>24</sup> The degree of depigmentation assessed was scored 2 weeks after treatment. The HC 100 mg/kg group showed skin melanin pigmentation was significantly developed compared to the vehicle and 8-MOP groups (Fig. 4C). The dorsal skin of C57BL/6 mice that received 5% HQ exposed significant pathological injury and epidermal thickening, as shown in H&E staining (Fig. 5A, B). To further assess the HC-treated melanogenic effect in our investigation, we examined the melanin content and tyrosinase activity of mouse skin samples receiving the HC treatment group, which increased significantly as compared to the vehicle and other treatment groups and were consistent with the results in vitro (Fig 5C, D).

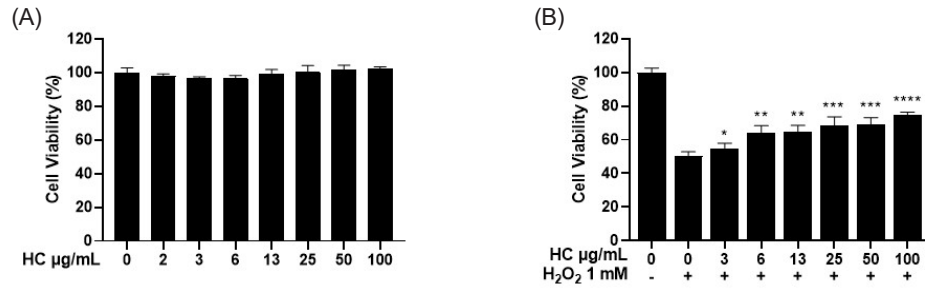


**Fig. 1.** Cell viability of the B16F10 melanoma cell. (A) Effects of different concentrations of HC. (B) Cells were pretreated with different concentrations of HC for 24 h and then exposed to 1 mM H<sub>2</sub>O<sub>2</sub> for 4 h. All the data are presented as the mean ± SD across (n = 9). \**p* < 0.05, \*\**p* < 0.01, \*\*\**p* < 0.005, \*\*\*\**p* < 0.001 indicate significant differences between the treated group and the H<sub>2</sub>O<sub>2</sub>-induced oxidative control.

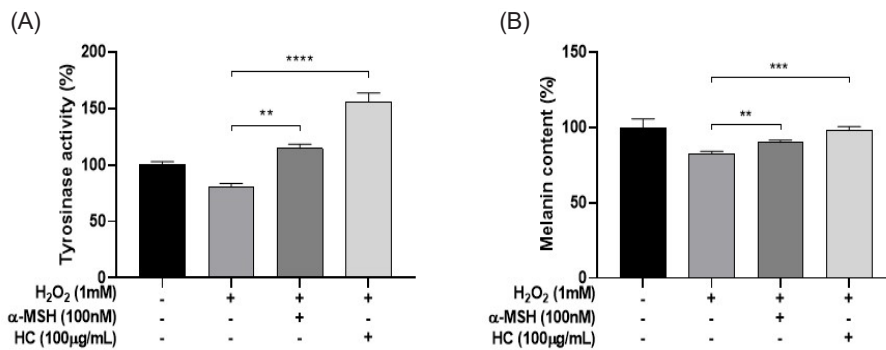


**Fig. 2.** Effects of HC on the melanin content and tyrosinase activity in B16F10 melanoma cells. HC was pretreated for 24 h and then stimulated with 1 mM H<sub>2</sub>O<sub>2</sub> for 4 h. The (A) tyrosinase activity and (B) melanin content were measured using a microplate reader. α-MSH was used as the positive control. Data are presented as mean ± SD (n = 3). \*\**p* < 0.01, \*\*\**p* < 0.005, and \*\*\*\**p* < 0.001 indicate significant differences between the HC-treated groups and the α-MSH group.

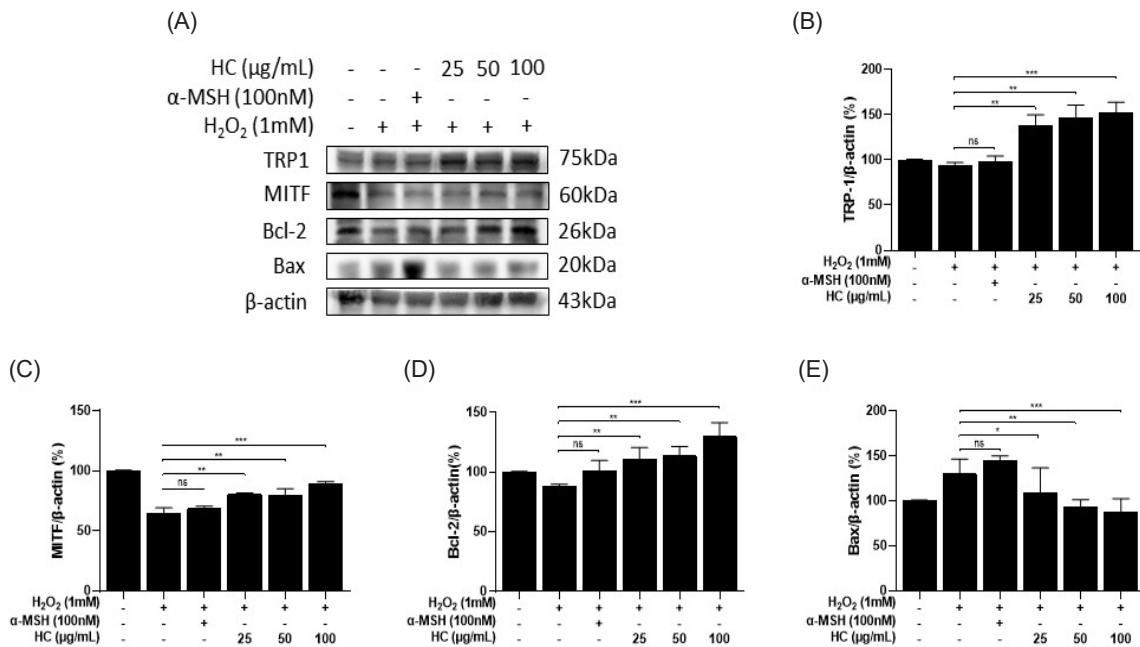


**Fig. 3.** HC enhances melanogenesis and anti-apoptotic expression in melanocytes. B16F10 cells were exposed to 25, 50, and 100 µg/mL of HC for 24 h and were induced with 1 mM H<sub>2</sub>O<sub>2</sub> for 4 h. (A) The levels of TRP-1, MITF, Bcl-2, and Bax expressions were determined by western blotting. (B–E) Quantitative analysis of melanin synthesis-related and apoptosis-regulating protein expression. α-MSH was used as the positive control. Results are presented as the mean ± SD across (n = 3). \**p* < 0.05; \*\**p* < 0.01, \*\*\**p* < 0.005; ns means no significance.

Melanin pigment's abnormal loss and destruction cause skin disorders with depigmented patches, such as vitiligo.<sup>25</sup> Oxidative stress is regarded as one of the possible pathogenic processes causing melanocyte loss. The deficient circulation of tetrahydrobiopterin in the epidermis of vitiligo patients may be highly related to intracellular H<sub>2</sub>O<sub>2</sub> generation.<sup>26</sup> ROS levels increasing in melanocytes produce defective apoptosis, promoting the provision of abnormal proteins as self-antigens, leading to autoimmunity.<sup>27</sup> However, in the present study, we investigated the in vivo and in vitro melanogenic effects of HC and found that it reduced H<sub>2</sub>O<sub>2</sub> oxidative stress-induced apoptosis in melanocytes. The Bcl-2 family, which includes the antiapoptotic protein Bcl-2 and the proapoptotic protein Bax, is crucial in the regulation of apoptosis.<sup>28</sup> Pretreatment with HC inhibits the expression of Bax and increases the Bcl-2 protein.

The transcriptional regulation of MITF, a master regulator of skin pigmentation, is responsible for the catalysis of melanin formation by the TRP-1 protein.<sup>29,30</sup> Our study determined that HC could significantly increase tyrosinase activity and melanin content at 100 g/mL concentrations in B16F10 cells under H<sub>2</sub>O<sub>2</sub>-induced oxidative stress. HC significantly increases the melanogenic enzymes TRP-1 and MITF expression levels

at 25, 50, and 100 µg/mL concentrations in B16F10 cells. Melanogenesis is a highly intricate cascade reaction in which the regulation of MITF and TYR expression affects over 255 genes.<sup>31</sup> These results suggest that under H<sub>2</sub>O<sub>2</sub>-induced oxidative stress on B16F10 melanocyte cells, the potential effect of HC promotes melanin synthesis and protection from apoptosis.

An animal model was utilized to confirm the potential medicinal benefits of HC in treating hypopigmentation disease. HQ-induced depigmentation in C57BL/6 mice reproduced this characteristic. As a result, we decided to investigate how HC affects melanogenesis using this model. During the third week of the experiment, the dorsal skin and hair of the HQ model mice were noticeably whitening. Otherwise, HC-treatment groups showed that the dorsal skin and hair were gradually darker. The H&E staining examined the distribution of melanin particles and the epidermal thickness of the mice. Our findings demonstrated that in vitiligo, the epidermal thickness contributes to the depigmentation.<sup>32,33</sup> Based on these reports, the HC has significant potential to reverse this phenomenon, which indicates that it inhibits the epidermal thickening induced by HQ.

In conclusion, these results indicate HC has the potential for vitiligo treatment and the protective effects of the injury induced

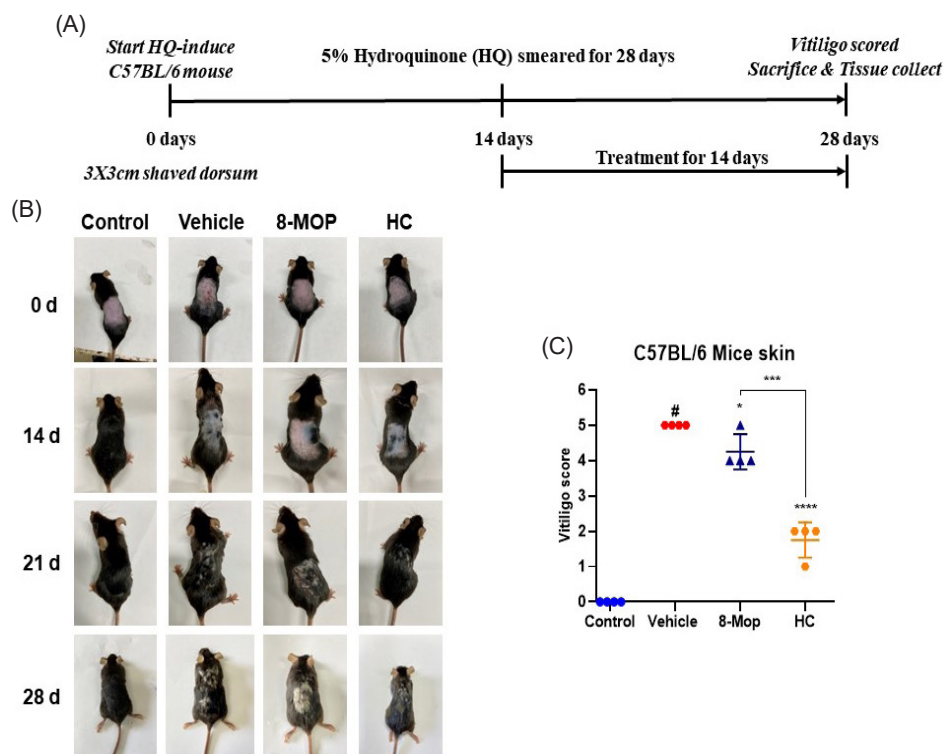


**Fig. 4.** C57BL/6 mouse model of hydroquinone-induced vitiligo. (A) Vitiligo-induced protocol and timeline. (B) Effect of HC on C57BL/6 mouse-induced vitiligo; presentation of control, vehicle, 8-MOP, and HC groups, respectively. (C) The vitiligo score was blind after 28 days. All data are presented as the mean ± SD across ( $n = 4$ ). \* $p < 0.05$ , \*\*\* $p < 0.005$ , and \*\*\*\* $p < 0.001$  indicate significant differences between the HC-treated group and the positive control group.

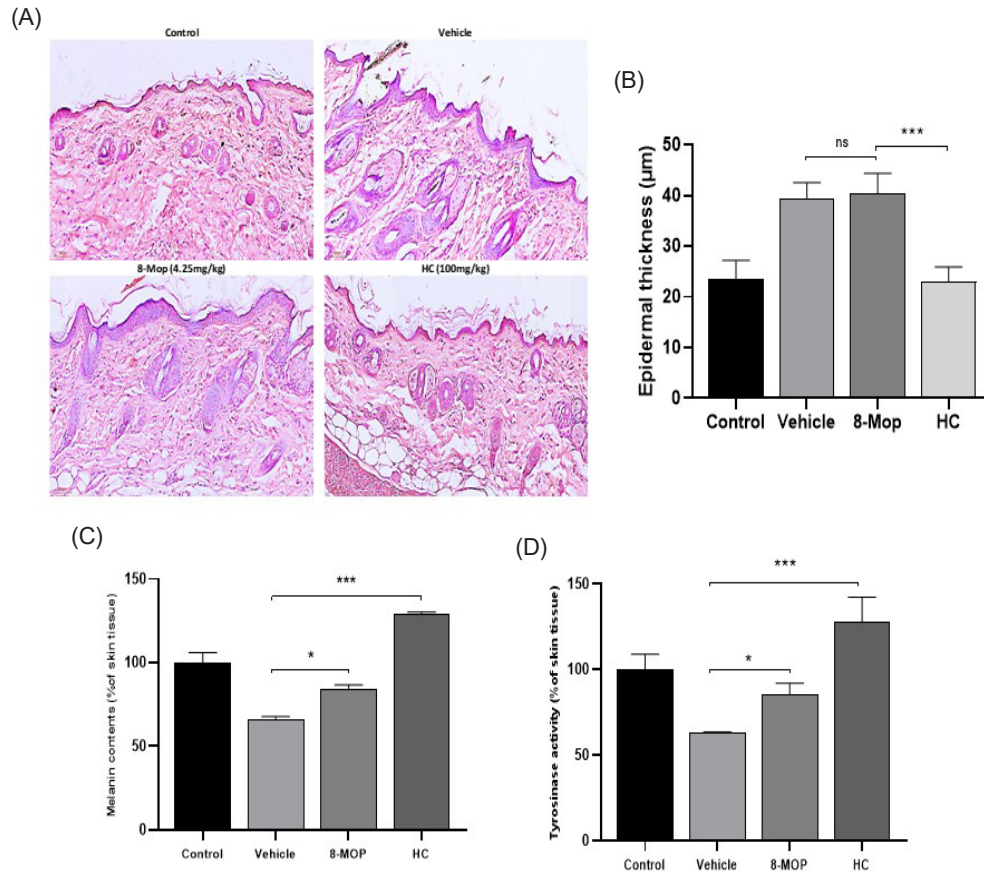


**Fig. 5.** The effects of HC on C57BL/6 mice subjected to experimental vitiligo-dorsal skin tissue. All tissues were stained with hematoxylin and eosin (H&E), and images were captured at 20 × magnification. (A) The photomicrograph shows the histological cross-section of the mouse dorsal skin. (B) Mice dorsal skin tissue epidermis thickness was measured. (C) The melanin content and (D) tyrosinase activity in skin tissue were measured using a microplate reader. The results are presented as the mean ± SD across ( $n = 4$ ). \* $p < 0.05$ ; \*\*\* $p < 0.005$ ; ns means no significance. Indicates significant differences between the HC-treated group and other treatment groups.

by oxidative stress *in vivo* and *in vitro*. Additionally, the HC stimulated melanin production and tyrosinase, increasing the melanogenesis expression of TRP-1, MITF, and anti-apoptotic effects. Oral administration of HC reduced the depigmentation of HQ-induced vitiligo by increasing the melanocytes. Furthermore, our research explored HC and the effect of the primary component of the extract on melanin, providing more research bases and new directions for drug development for HC in the treatment of depigmented skin diseases such as vitiligo.

### Acknowledgments

This research was supported by Basic Science Research Program through the National Research Foundation of Korea (NRF), funded by the Ministry of Education (NRF-2021R111A3055927 to Soh Y), and the Research Base Construction Fund Support Program funded by Jeonbuk National University in 2024. This paper was also supported by a grant from

the Technology Innovation Program (20012892) funded by the Ministry of Trade, Industry & Energy (MOTIE, Korea).

### Conflicts of Interest

The authors declare that there is no conflict of interest.

### References

- (1) Whitton, M. E.; Pinart, M.; Batchelor, J.; Leonardi-Bee, J.; Gonzalez, U.; Jiyad, Z.; Eleftheriadou, V.; Ezzedine, K. J. *Cochrane Database Syst. Rev.* **2015**, *2015*, CD003263.
- (2) Zhang, Y.; Cai, Y.; Shi, M.; Jiang, S.; Cui, S.; Wu, Y.; Gao, X.-H.; Chen, H.-D. *J. PLoS One* **2016**, *11*, e0163806.
- (3) Alikhan, A.; Felsten, L. M.; Daly, M.; Petronic-Rosic, V. *J. Am. Acad. Dermatol.* **2011**, *65*, 473–491.
- (4) Hearing, V. J. *J. Dermatol. Sci.* **2005**, *37*, 3–14.
- (5) Chang, W.-L.; Ko, C.-H. *Cells* **2023**, *12*, 936.
- (6) Manga, P.; Elbuluk, N.; Orlow, S. J. *F1000Res.* **2016**, *5*, 1–9.
- (7) Slominski, A.; Tobin, D. J.; Shibahara, S.; Wortsman, J. *Physiol. Rev.* **2004**, *84*, 1155–1228.
- (8) Zhang, X.; Li, J.; Li, Y.; Liu, Z.; Lin, Y.; Huang, J.-A. *Fitoterapia* **2020**,

- 145, 104634.
- (9) Möller, K.; Sigurbjörnsdóttir, S.; Arnthorsson, A. O.; Pogenberg, V.; Dilshat, R.; Fock, V.; Brynjólfsdóttir, S. H.; Bindesboll, C.; Bessadóttir, M.; Ogmundsdóttir, M. H. *Sci. Rep.* **2019**, *9*, 1055.
- (10) Vachtenheim, J.; Borovanský, J. *Exp. Dermatol.* **2010**, *19*, 617–627.
- (11) Van Den Wijngaard, R. M.; Aten, J.; Scheepmaker, A.; Le Poole, I. C.; Tigges, A. J.; Westerhof, W.; Das, P. K. *Br. J. Dermatol.* **2000**, *143*, 573–581.
- (12) Kowaltowski, A. J.; Fenton, R. G.; Fiskum, G. *Free Radic. Biol. Med.* **2004**, *37*, 1845–1853.
- (13) Zhou, J.; Feng, J.-Y.; Wang, Q.; Shang, J. *Cytokine* **2015**, *74*, 137–144.
- (14) Xuan, Y.; Yang, Y.; Xiang, L.; Zhang, C. *Oxid. Med. Cell Longev.* **2022**, *2022*, 8498472.
- (15) Yang, L.; Jiang, J.-G. *Pharm. Biol.* **2009**, *47*, 1154–1161.
- (16) Li, W.; Zhou, P.; Zhang, Y.; He, L. *J. Ethnopharmacol.* **2011**, *133*, 922–927.
- (17) Wei, P.; Luo, Q.; Hou, Y.; Zhao, F.; Li, F.; Meng, Q. *Phytomedicine* **2023**, *123*, 155195.
- (18) Bae, J.-S.; Han, M.; Yao, C.; Chung, J. H. *Chem. Biol. Interact.* **2016**, *245*, 66–71.
- (19) Kim, A.; Yim, N.-H.; Im, M.; Jung, Y. P.; Liang, C.; Cho, W.-K.; Ma, J. Y. *BMC Complement. Altern. Med.* **2013**, *13*, 1–10.
- (20) Lee, Y.; Hwang, K. *Surg. Radiol. Anat.* **2002**, *24*, 183–189.
- (21) Curtis, A.; Calabro, K.; Galarneau, J.-R.; Bigio, I. J.; Krucker, T. *Mol. Imaging Biol.* **2011**, *13*, 1114–1123.
- (22) Kwon, S.; Sevic-Muraca, E. M. *Contrast Media Mol. Imaging.* **2017**, *2017*, 7659242.
- (23) Na, J.-I.; Shin, J.-W.; Choi, H.-R.; Kwon, S.-H.; Park, K.-C. *Int. J. Mol. Sci.* **2019**, *20*, 956.
- (24) Zang, D.; Niu, C.; Lu, X.; Aisa, H. A. *Int. J. Mol. Sci.* **2022**, *23*, 14190.
- (25) Zang, D.; Niu, C.; Aisa, H. A. *Drug Des. Devel. Ther.* **2019**, 623–632.
- (26) Laddha, N. C.; Dwivedi, M.; Mansuri, M. S.; Gani, A. R.; Ansarullah, M.; Ramachandran, A.; Dalai, S.; Begum, R. *Exp. Dermatol.* **2013**, *22*, 245–250.
- (27) Kuhlreiber, W. M.; Hayashi, T.; Dale, E. A.; Faustman, D. L. *J. Mol. Endocrinol.* **2003**, *31*, 373–399.
- (28) Jiang, W.; Li, S.; Chen, X.; Zhang, W.; Chang, Y.; He, Y.; Zhang, S.; Su, X.; Gao, T.; Li, C.; Jian, Z. *J. Dermatol. Sci.* **2019**, *94*, 236–243.
- (29) Ullah, S.; Park, C.; Ikram, M.; Kang, D.; Lee, S.; Yang, J.; Park, Y.; Yoon, S.; Chun, P.; Moon, H. R. *Bioorg. Chem.* **2019**, *87*, 43–55.
- (30) Levy, C.; Khaled, M.; Fisher, D. E. *Trends. Mol. Med.* **2006**, *12*, 406–414.
- (31) Hearing, V. J. *J. Invest. Dermatol.* **2011**, *131*, E1.
- (32) Slominski, A.; Paus, R.; Costantino, R. J. *J. Invest. Dermatol.* **1991**, *96*, 172–179.
- (33) Bastonini, E.; Kovacs, D.; Picardo, M. *Ann. Dermatol.* **2016**, *28*, 279–289.

Received July 31, 2024

Revised August 31, 2024

Accepted September 19, 2024